Co-Construction of Sulfur Vacancies and Heterogeneous Interface into Ni_3S_2/MoS_2 Catalysts to Achieve Highly Efficient Overall Water Splitting

Zhaoyang An[1], Hui Xue[1]*, Jing Sun[1], Niankun Guo[1], Tianshan Song[1], Jiawen Sun[1], Yi-Ru Hao[1] and Qin Wang[1]*

[1]College of Chemistry and Chemical Engineering, Inner Mongolia University, Hohhot 010021 China

**Corresponding authors. Emails: qinwang@imu.edu.cn (Q. Wang) and hxue@imu.edu.cn (H. Xue)*

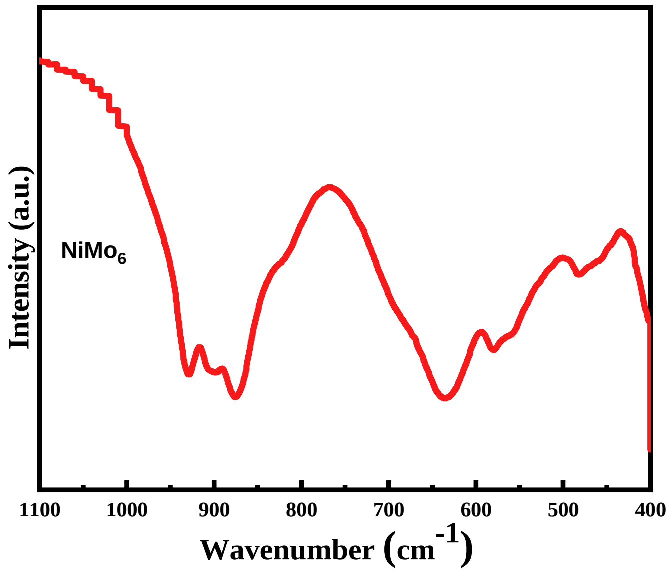

Figure S1. FT-IR spectrum of $NiMo_6$.

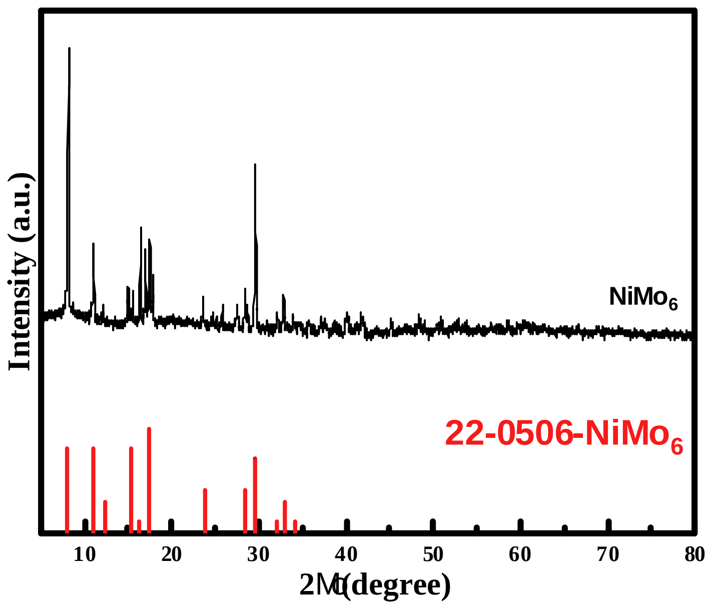

Figure S2. XRD patterns of $NiMo_6$.

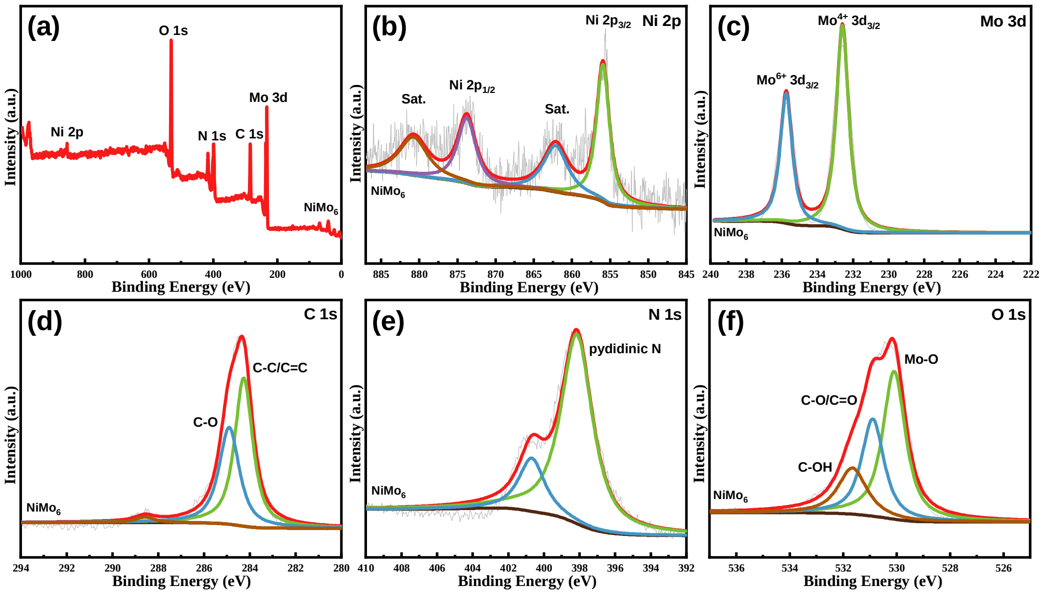

Figure S3. XPS spectra of $NiMo_6$: (a) XPS survey, (b) Ni 2p, (c) Mo 3d, (d) C 1s, (e) N 1s, and (f) O 1s.

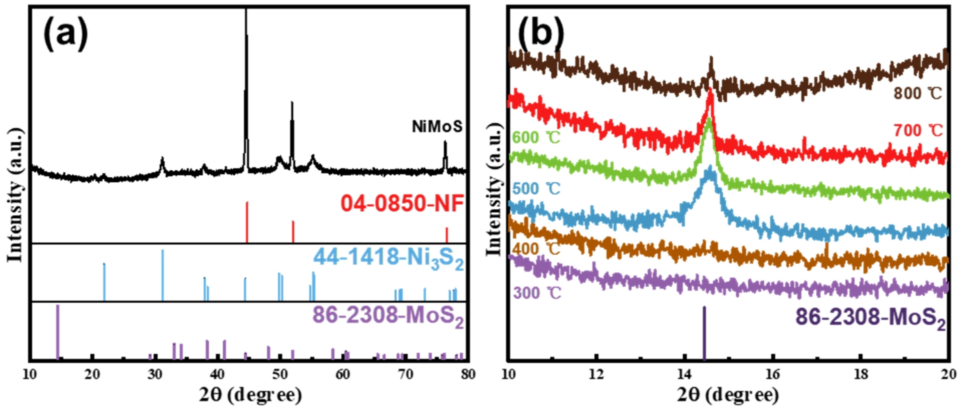

Figure S4. (a) XRD patterns of NiMoS; (b) XRD patterns of the V_S-Ni_3S_2/MoS_2 catalysts in a 2θ range of 10-20°.

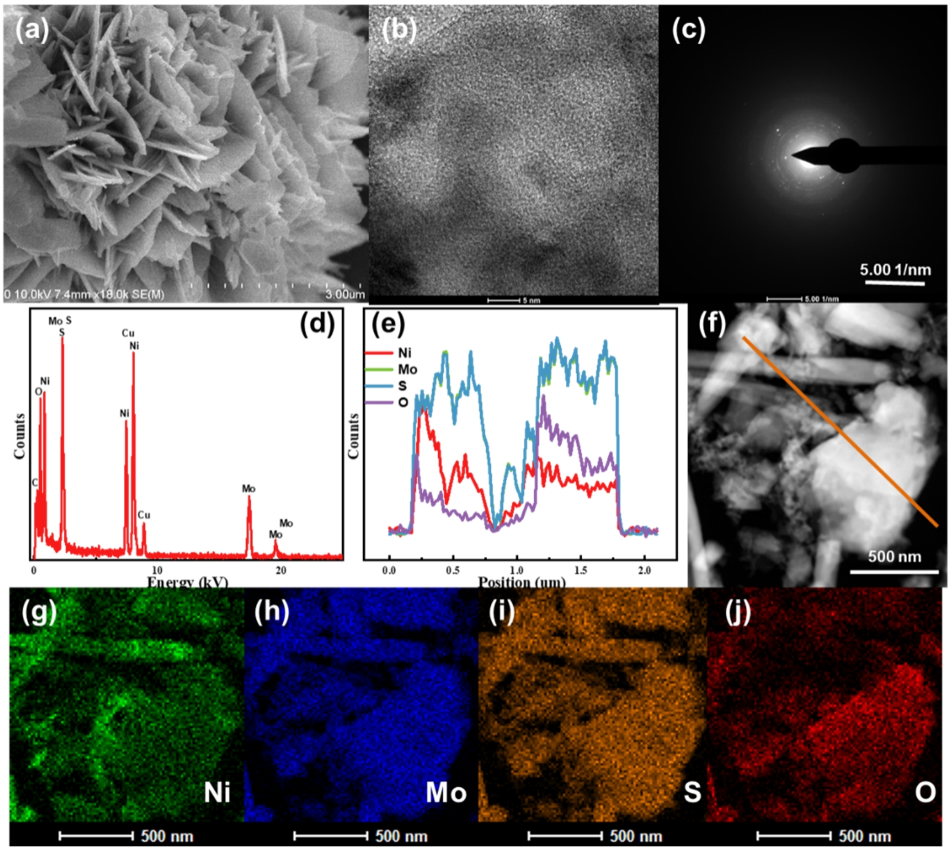

Figure S5. (a) SEM image of NiMoS; (b) HRTEM image; (c) SAED pattern; (d) EDX spectra; (e) The line scanning profiles of Ni, Mo, S and O recorded along the line shown in (f); (f) HAADF-STEM; (g-j) The element mapping results of NiMoS.

The line scanning profiles recorded have been shown in Figure 1g and Figure S6. And the lines of sulfur (blue) and molybdenum (green) roughly coincide.

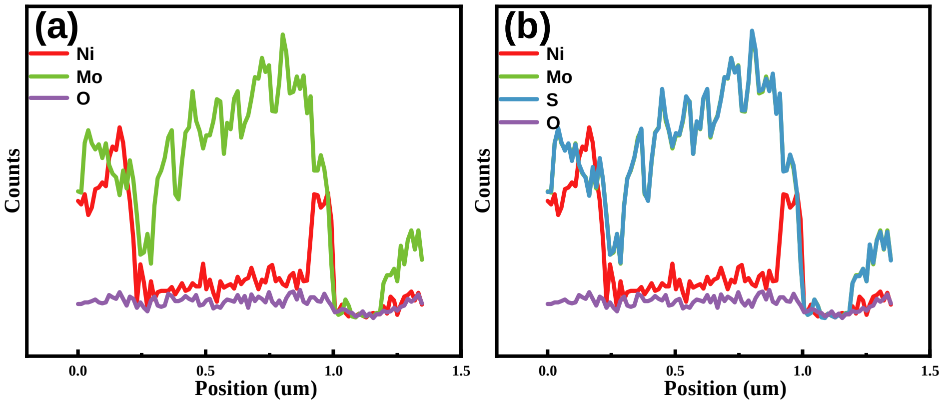

Figure S6. The line scanning profiles of (a) Ni, Mo, and O, (b) Ni, Mo, S, and O recorded along the line shown in Figure 1(f).

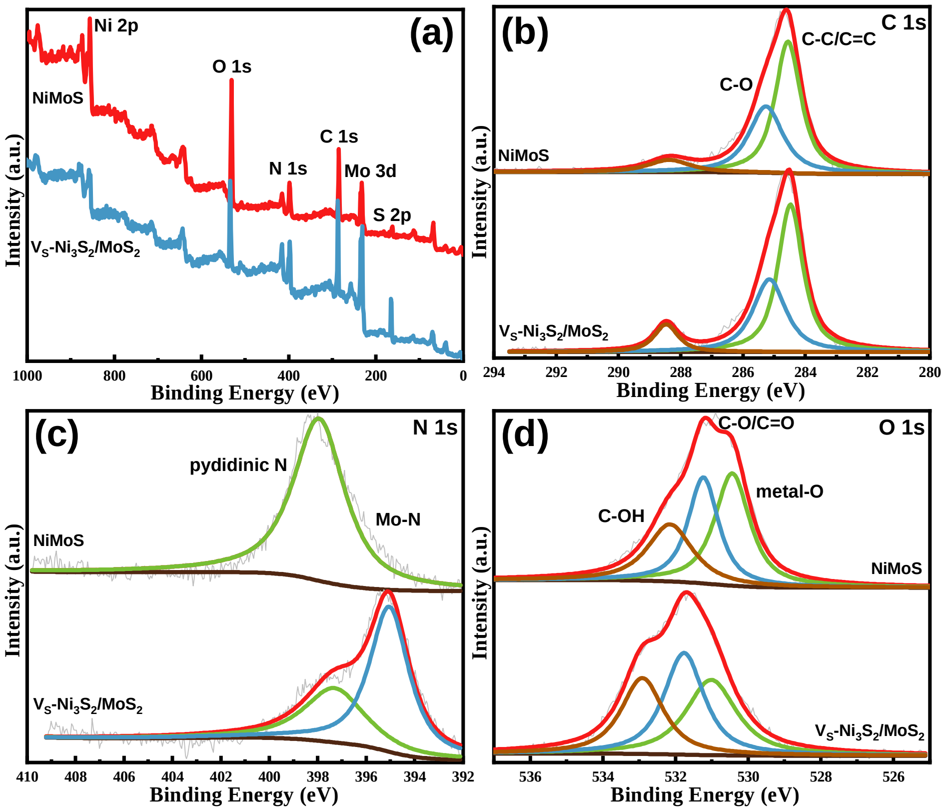

Figure S7. XPS spectra of the NiMoS and V_S-Ni_3S_2/MoS_2 catalysts: (a) XPS survey, (b) C 1s, (c) N 1s, and (d) O 1s.

The Raman spectra of NiMoS and V_S-Ni_3S_2/MoS_2 catalysts are presented in Figure S8. The Raman scattering shows that NiMoS has no obvious scattering peak at 360-430 cm^{-1}, but the peaks corresponding to the V_S-Ni_3S_2/MoS_2 become more obvious after being reduced by hydrogen.[1]

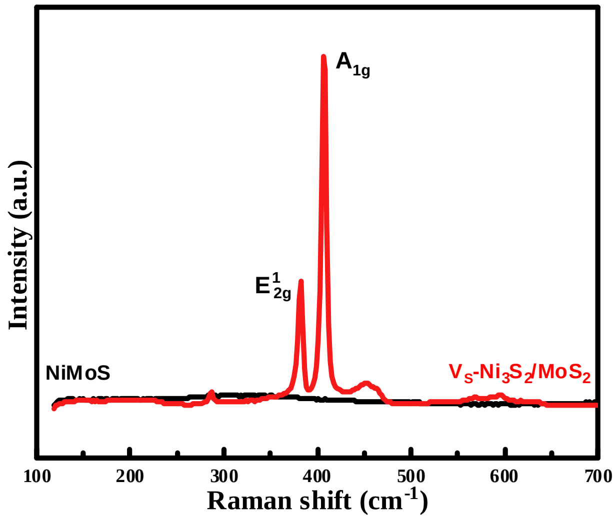

Figure S8. Raman spectra of the NiMoS and V_S-Ni_3S_2/MoS_2 catalysts.

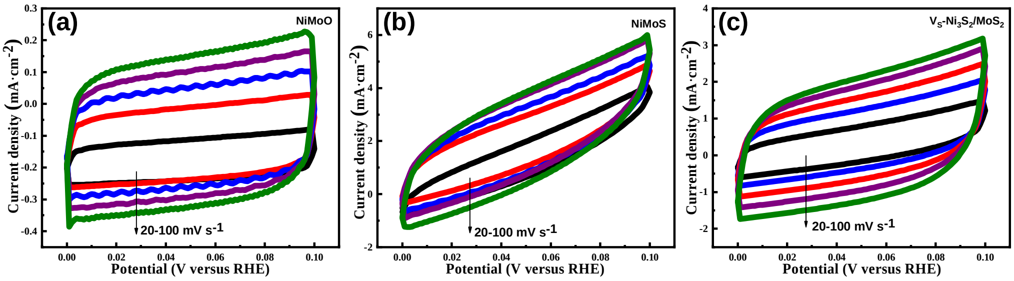

Figure S9. CVs of the various catalysts at the different scan rates from 20 to 100 mV·s^{-1}: (a) NiMoO, (b) NiMoS, and (c) V_S-Ni_3S_2/MoS_2.

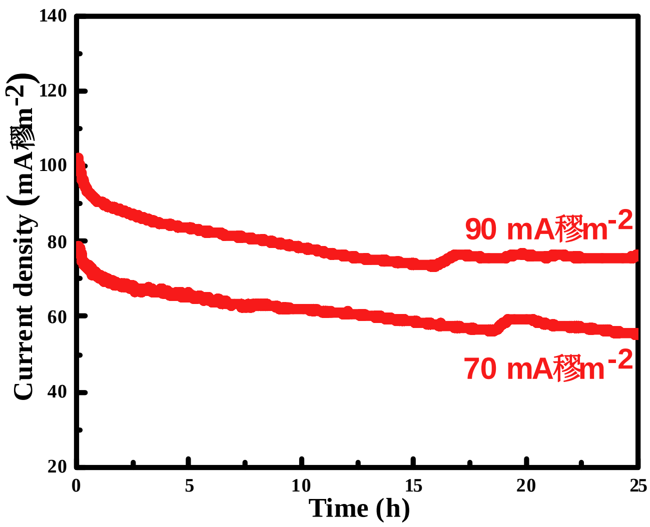

Figure S10. The chronopotentiometric durability test of the catalysts.

Chinese Journal of Structural Chemistry

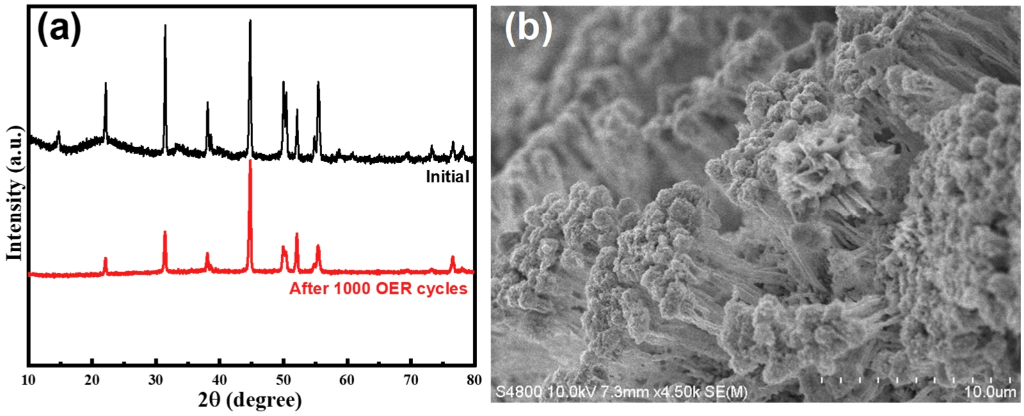

Figure S11. After 1000 OER cycles: (a) XRD patterns and (b) SEM image.

After 1000 CV cycles, the XRD and SEM images are roughly similar to the initial patterns, but the peak of MoS_2 disappears (Figure S11). It is speculated that a large number of tetravalent Mo (IV) are oxidized to hexavalent Mo (VI), which can be demonstrated from the Mo 3d XPS spectra after 1000 CV cycles in Figure S12b.

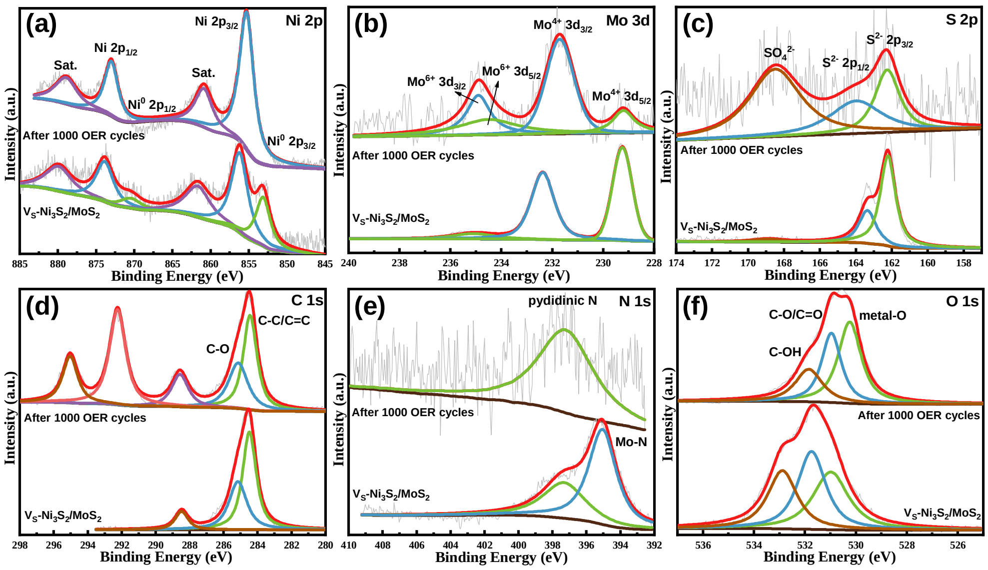

Figure S12. XPS spectra of the V_S-Ni_3S_2/MoS_2 catalysts after 1000 OER cycles: (a) Ni 2p, (b) Mo 3d, (c) S 2p, (d) C 1s, (e) N 1s, and (f) O 1s.

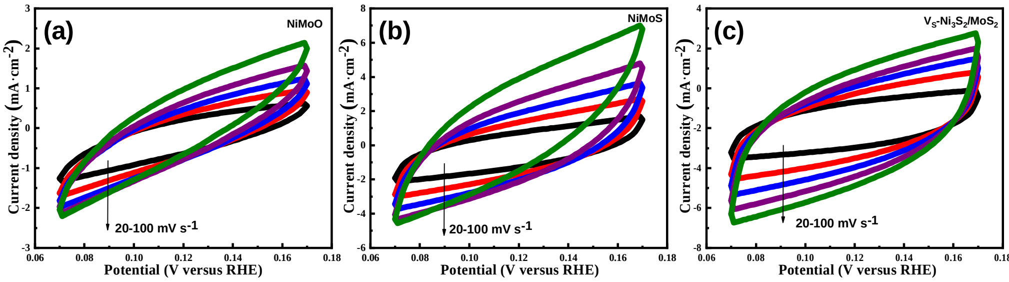

Figure S13. CVs of the various catalysts at the different scan rates from 20 to 100 mV·s^{-1}: (a) NiMoO, (b) NiMoS, and (c) V_S-Ni_3S_2/MoS_2.

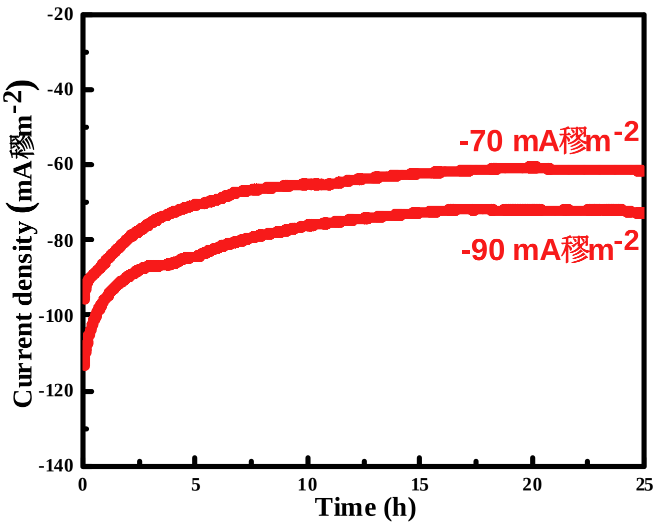

Figure S14. The chronopotentiometric durability test of the catalysts.

Chinese Journal of Structural Chemistry

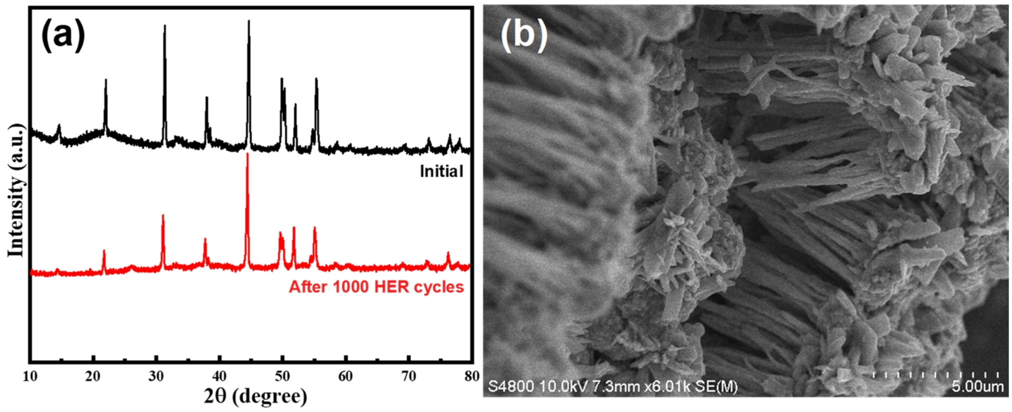

Figure S15. After 1000 HER cycles: (a) XRD patterns and (b) SEM image.

The 1000 CV cycles results reveal outstanding HER stability for the V_S-Ni_3S_2/MoS_2 catalysts. And after 1000 CV cycles, the XRD, SEM, and XPS spectra of V_S-Ni_3S_2/MoS_2 catalysts are roughly similar to the initial sample (Figure S15-16).

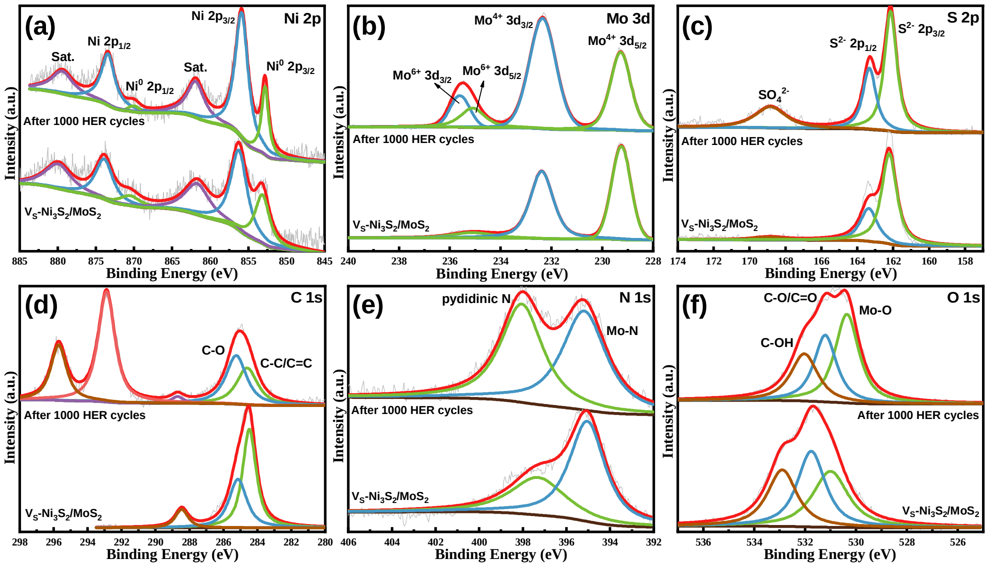

Figure S16. XPS spectra of the V_S-Ni_3S_2/MoS_2 catalysts after 1000 HER cycles: (a) Ni 2p, (b) Mo 3d, (c) S 2p, (d) C 1s, (e) N 1s, and (f) O 1s.

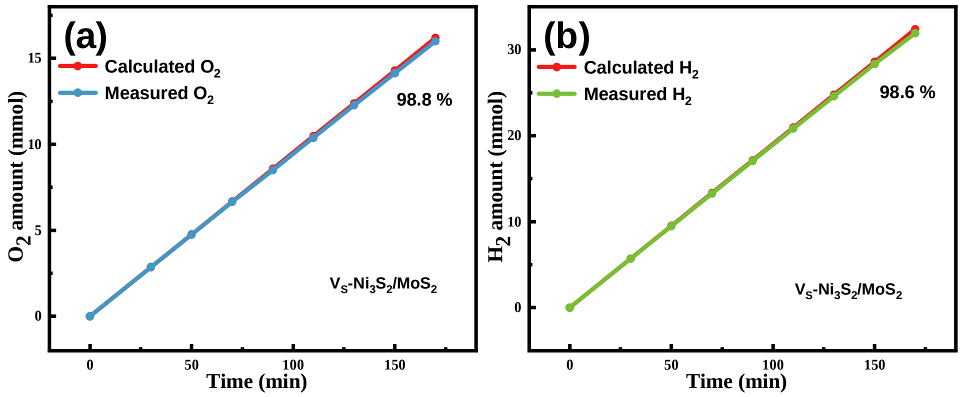

Figure S17. Faraday efficiency of the V_S-Ni_3S_2/MoS_2 catalysts: (a) OER and (b) HER.

Table S1. Proportion of Each Element of the V_S-Ni_3S_2/MoS_2 Catalysts

Element	Ni	Mo	S	C	N	O
Proportion	4.19%	6.55%	8.44%	43.71%	19.08%	18.02%

Table S2. Comparison of OER Electrocatalytic Activity of Samples Reported in This Work and Some Representative Catalysts That Have Been Recently Reported in Alkaline Medium

Catalysts	Current density ($mA \cdot cm^{-2}$)	Overpotential (mV)	Electrolyte	Reference
V_S-Ni_3S_2/MoS_2	**10**	**180**	**1.0 M KOH**	**This work**
MoS_2/LDH	10	210	1.0 M KOH	Nano Lett. 2019, 19, 4518.
Ni/Mo_2C-NCNFs	10	288	1.0 M KOH	Adv. Energy Mater. 2019, 9, 1803185.
Co-MoS/CC	10	300	1.0 M KOH	Nanoscale, 2018, 10, 8404–8412.
Ni_3S_2/NF	10	260	1.0 M KOH	J. Am. Chem. Soc. 2015, 137, 14023-14026.
$Fe_{0.09}Co_{0.13}$-$NiSe_2$	10	251	1.0 M KOH	Adv. Mater. 2018, 30, 1802121.
CoMoNiS-NF-31	100	260	1.0 M KOH	J. Am. Chem. Soc. 2019, 141, 10417.
MoOx/Ni_3S_2	100	310	1.0 M KOH	Adv. Funct. Mater. 2016, 26, 4839.
Fe-Ni_3S_2/FeNi	100	500	1.0 M KOH	Small 2017, 13, 1604161.
$Fe_{0.9}Ni_{2.1}S_2$@NF	100	252	1.0 M KOH	Adv. Energy Mater. 2020, 10, 2001963.
Ni_3S_2@MoS_2/FeOOH	10	260	1.0 M KOH	Appl. Catal. B 2019, 244, 1004.
Ni-Mo-N/CFC	10	340	1.0 M KOH+0.1 M Gly	Nat. Commun. 2019, 10, 5335.
Fe-Ni@NC-CNTs	10	274	1.0 M KOH	Angew. Chem. 2018, 130, 9059.

Ni_3S_2/NF	10	270	1.0 M KOH+10 mM HMF	J. Am. Chem. Soc. 2016, 13639-13646.
Mo-CoOOH	10	305	1.0 M KOH	Nano Energy 2018, 48, 73.
MoS_2/Co_9S_8/Ni_3S_2/Ni	10	166	1.0 M KOH	J. Am. Chem. Soc. 2019, 141, 10417-10430.
CoS_2 NT	10	276	1.0 M KOH	Nanoscale Horiz. 2017, 2, 342—348.
NiTe/NiS	10	244	1.0 M KOH	Adv. Mater. 2019, 31, 1900430.
$CoNiPS_3$/C	10	262	1.0 M KOH	Adv. Mater. 2018, 28, 1805075.
NiMoOx/NiMoS	10	186	1.0 M KOH	Nat. Commun. 2020, 11, 5462.
Co-Ni_3N	10	307	1.0 M KOH	Adv. Mater. 2018, 30, 1705516.
Ni-Fe-MoN	10	288	1.0 M KOH	Adv. Energy Mater. 2018, 8, 1802327.
NiSe/NF	10	270	1.0 M KOH	Angew. Chem. Int. Ed. 2015, 54, 1.
Ni/NiFeMoOx/NF	10	255	1.0 M KOH	Adv. Sci. 2020, 7, 1902034.
NiS/NF	10	302	1.0 M KOH	Chem. Commun. 2016, 52, 1486.

Chinese Journal of Structural Chemistry

Table S3. Comparison of HER Electrocatalytic Activity of Samples Reported in This Work and Some Representative Catalysts That Have Been Recently Reported in Alkaline Medium

Catalysts	Current density ($mA \cdot cm^{-2}$)	Overpotential (mV)	Electrolyte	Reference
V_S-Ni_3S_2/MoS_2	**10**	**71**	**1.0 M KOH**	**This work**
C-MoS_2	10	45	1.0 M KOH	Nat. Commun. 2019, 10, 1217.
1T-MoS_2	10	46	1.0 M KOH	Nat. Commun. 2019, 10, 982.
NiFeS	10	180	1.0 M KOH	J. Mater. Chem. A 2016, 4, 16394.
Ni-MoS_2/CC	10	98	1.0 M KOH	Energy Environ. Sci. 2016, 9, 2789-2793.
3D Ni_3S_2	10	182	1.0 M KOH	J. Mater. Chem. A 2016, 4, 13916.
Mo-W-S-2@Ni_3S_2	10	98	1.0 M KOH	ACS Appl. Mater. Interfaces 2017, 9, 26066.
$NiCo_2S_4$@NiFe LDH	10	200	1.0 M KOH	ACS Appl. Mater. Interfaces 2017, 9, 15364.
MoS_2-Ni_3S_2 HNRs/NF	10	98	1.0 M KOH	ACS Catal. 2017, 7, 2357.
CuCo-Ni_3S_2	10	204	1.0 M KOH	Appl. Surf. Sci. 2020, 502, 144172.
$NiCo_2S_4$/Ni_3S_2	10	119	1.0 M KOH	ACS Appl. Mater. Interfaces 2018, 10, 10890.
$Ni_{0.2}Mo_{0.8}$N/Ni	10	14	1.0 M KOH	Energy Environ. Sci. 2020,13, 3007-3013.
$Ni(OH)_2$/MoS_2	10	80	1.0 M KOH	Nano Energy 2017, 37, 74–80.
Ni-Mo-N/CFC	10	43	1.0 M KOH+0.1 M Gly	Nat. Commun. 2019, 10, 5335.
TiO_2@Co_9S_8	10	139	1.0 M KOH	Adv. Sci. 2018, 5, 1700772.

Ni_3S_2/NF	10	160	1.0 M KOH+10 mM HMF	J. Am. Chem. Soc. 2016, 13639-13646.
N-Ni_3S_2	10	110	1.0 M KOH	Adv. Mater. 2017, 29, 1701584.
MoO_3/Ni-NiO	10	62	1.0 M KOH	Adv. Mater. 2020, 32, 2003414.
$CoNiPS_3$/C	10	136	1.0 M KOH	Adv. Mater. 2018, 28, 1805075.
O-CoMoS	10	97	1.0 M KOH	ACS Catal. 2018, 8, 4612-4621.
Ni_2P/Ni_3S_2	10	80	1.0 M KOH	Nano Energy 2018, 51, 26.
MoS_2/NiS_2	10	62	1.0 M KOH	Adv. Sci. 2019, 6, 1900246.
Ni_2P/Fe_2P	10	121	1.0 M KOH	Adv. Energy Mater. 2018, 8, 1800484.
NiMoOx/NiMoS	10	38	1.0 M KOH	Nat. Commun. 2020, 11, 5462.
NiSe/NF	10	96	1.0 M KOH	Angew. Chem. Int. Ed. 2015, 54, 1.

Table S4. Comparison of Overall Water Splitting Electrocatalytic Activity of Samples Reported in This Work and Some Representative Catalysts That Have Been Recently Reported in Alkaline Medium

Catalysts	Current density ($mA\cdot cm^{-2}$)	Overpotential (mV)	Electrolyte	Reference
V_S-Ni_3S_2/MoS_2	**10**	**1.46**	**1.0 M KOH**	**This work**
Ni/Mo_2C-NCNFs	10	1.64	1.0 M KOH	Adv. Energy Mater. 2019, 9, 1803185.
Ni/Ni$(OH)_2$	10	1.59	1.0 M KOH	Adv. Mater. 2020, 32, 1906915.
Co-Mo-S/CC	20	1.64	1.0 M KOH	Nanoscale, 2018,10, 8404-8412.
Mo-doped Ni_3S_2	10	1.53	1.0 M KOH	J. Mater. Chem. A 2017, 5, 1595.
Ni_3S_2	10	1.55	1.0 M KOH	J. Mater. Chem. A 2019, 7, 18003.
V-doped Ni_3S_2	10	1.55	1.0 M KOH	J. Mater. Chem. A 2019, 7, 18118.
$Ni_3(S_{0.25}Se_{0.75})_2$@NiOOH	10	1.55	1.0 M KOH	Small 2018, 14, 1803666.
NiFe/(Ni, Fe)$_3S_2$	10	1.56	1.0 M KOH	Small Methods 2019, 3, 1900234.
MoS_2/Ni_3S_2	10	1.56	1.0 M KOH	Angew. Chem. Int. Ed. 2016, 55, 6702.
Ni_3S_2/VS_4 nanohorn	10	1.57	1.0 M KOH	Appl. Catal. B: Environ. 2019, 257, 117911.
Ni$(OH)_2$/Ni_3S_2-12 h	10	1.57	1.0 M KOH	J. Mater. Chem. A 2018, 6, 6938.
Ni_3S_2-NGQDs/NF	10	1.58	1.0 M KOH	Small 2017, 13, 1700264.
$NiCo_2S_4$@NiFe LDH	10	1.6	1.0 M KOH	ACS Appl. Mater. Interfaces 2017, 9, 15364.

$Fe_{11.1\%}$-Ni_3S_2	10	1.6	1.0 M KOH	J. Mater. Chem. A 2018, 6, 4346.
Mo-W-S-2@Ni_3S_2	10	1.62	1.0 M KOH	ACS Appl. Mater. Interfaces 2017, 9, 26066.
Co_9S_8/Ni_3S_2	10	1.64	1.0 M KOH	Appl. Catal. B: Environ. 2019, 253, 246.
Ni_3S_2	10	1.76	1.0 M KOH	J. Mater. Chem. A 2018, 6, 19201.
CuCo-Ni_3S_2	10	1.572	1.0 M KOH	Appl. Surf. Sci. 2020, 502, 144172.
Ni_3S_2 NTFs	10	1.611	1.0 M KOH	Appl. Catal. B: Environ. 2019, 243, 693.
NiMoS	10	1.53	1.0 M KOH	Appl. Catal. B: Environ. 2020, 268, 118435.
$Fe_{0.9}Ni_{2.1}S_2$@NF	10	1.51	1.0 M KOH	Adv. Energy Mater. 2020, 10, 2001963.
NiFe-NiMo/Ni-P	10	1.51	1.0 M KOH	Nat. Commun. 2018, 9, 2014.
CoMoNiS-NF	10	1.54	1.0 M KOH	J. Am. Chem. Soc. 2019, 141, 10417-10430.
Ni_3S_2	10	1.76	1.0 M KOH	J. Am. Chem. Soc. 2015, 137, 14023-14026.
MoO_3/Ni-NiO	10	1.55	1.0 M KOH	Adv. Mater. 2020, 32, 2003414.
Se-(NiCo)S/OH	10	1.6	1.0 M KOH	Adv. Mater. 2018, 30, 1705538.
Co-MoS_2/BCCF	10	1.55	1.0 M KOH	Adv. Mater. 2018, 30, 1801450.
Fe-Ni-MoN	10	1.51	1.0 M KOH	Adv. Energy Mater. 2018, 8, 1802327.
N-$NiMoO_4$/NiS_2	10	1.6	1.0 M KOH	Adv. Funct. Mater. 2019, 29, 1805298.

$NiCo_2S_4$	10	1.68	1.0 M KOH	Adv. Funct. Mater. 2016, 26, 4661-4672.
O-CoMoS	10	1.6	1.0 M KOH	ACS Catal. 2018, 8, 4612-4621.
NiMoOx/NiMoS	10	1.46	1.0 M KOH	Nat. Commun. 2020, 11, 5462.

n REFERENCES

(1) Li, Y.; Qian, J.; Zhang, M. H.; Wu, C. Co-construction of sulfur vacancies and heterojunctions in tungsten disulfide to induce fast electronic/ionic diffusion kinetics for sodium-ion batteries. *Adv. Mater.* **2020**, 32, 2005802.